Science of the Total Environment 550 (2016) 103–113

Contents lists available at ScienceDirect

Science of the Total Environment

journal homepage: www.elsevier.com/locate/scitotenv

Molybdenum and zinc stable isotope variation in mining waste rock drainage and waste rock at the Antamina mine, Peru

E.K. Skierszkan [a,*], K.U. Mayer [a], D. Weis [b], R.D. Beckie [a]

[a] Department of Earth, Ocean and Atmospheric Sciences, University of British Columbia, 2020-2207 Main Mall, Vancouver V6T 1Z4, Canada
[b] Pacific Centre for Isotopic and Geochemical Research (PCIGR), Department of Earth, Ocean and Atmospheric Sciences, University of British Columbia, 2020-2207 Main Mall, Vancouver V6T 1Z4, Canada

HIGHLIGHTS

- Metal stable isotopes are promising indicators of attenuation in mine drainage.
- Mine water, waste rock and minerals were analyzed for Mo and Zn isotope ratios.
- Molybdenites had a wide range of δ^{98}Mo, but sphalerites had invariant δ^{66}Zn.
- Variations of 2.2‰ in δ^{98}Mo and 0.7‰ in δ^{66}Zn were measured in mine drainage.
- Attenuation processes drive changes in δ^{66}Zn and δ^{98}Mo in solution.

GRAPHICAL ABSTRACT

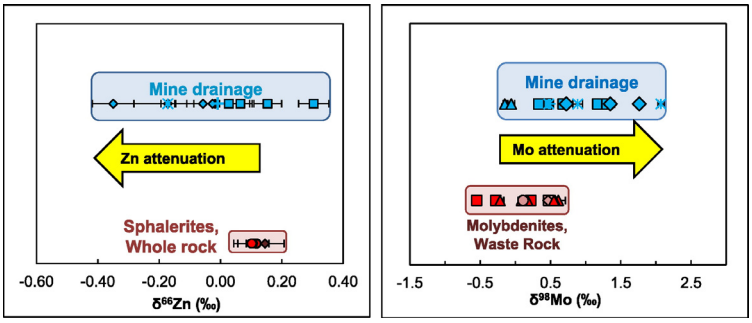

ARTICLE INFO

Article history:
Received 9 October 2015
Received in revised form 10 January 2016
Accepted 10 January 2016
Available online xxxx

Editor: D. Barcelo

Keywords:
Heavy stable isotopes
Mine drainage
Multicollector ICP-MS
Molybdenum
Zinc

ABSTRACT

The stable isotope composition of molybdenum (Mo) and zinc (Zn) in mine wastes at the Antamina Copper–Zn–Mo mine, Peru, was characterized to investigate whether isotopic variation of these elements indicated metal attenuation processes in mine drainage. Waste rock and ore minerals were analyzed to identify the isotopic composition of Mo and Zn sources, namely molybdenites (MoS_2) and sphalerites (ZnS). Molybdenum and Zn stable isotope ratios are reported relative to the NIST-SRM-3134 and PCIGR-1 Zn standards, respectively. δ^{98}Mo among molybdenites ranged from −0.6 to +0.6‰ (n = 9) while sphalerites showed no δ^{66}Zn variations (0.11 ± 0.01‰, 2 SD, n = 5). Mine drainage samples from field waste rock weathering experiments were also analyzed to examine the extent of isotopic variability in the dissolved phase. Variations spanned 2.2‰ in δ^{98}Mo (−0.1 to +2.1‰) and 0.7‰ in δ^{66}Zn (−0.4 to +0.3‰) in mine drainage over a wide pH range (pH 2.2–8.6). Lighter δ^{66}Zn signatures were observed in alkaline pH conditions, which was consistent with Zn adsorption and/or hydrozincite ($Zn_5(OH)_6(CO_3)_2$) formation. However, in acidic mine drainage Zn isotopic compositions reflected the value of sphalerites. In addition, molybdenum isotope compositions in mine drainage were shifted towards heavier values (0.89 ± 1.25‰, 2 SD, n = 16), with some overlap, in comparison to molybdenites and waste rock (0.13 ± 0.82‰, 2 SD, n = 9). The cause of heavy Mo isotopic signatures in mine drainage was more difficult to resolve due to isotopic heterogeneity among ore minerals and a variety of possible overlapping processes including dissolution, adsorption and secondary mineral precipitation. This study shows that variation in metal isotope ratios are promising indicators of metal attenuation. Future characterization of isotopic fractionation associated to key environmental reactions will improve the power of Mo and Zn isotope ratios to track the fate of these elements in mine drainage.

* Corresponding author.
E-mail address: eskiersz@eos.ubc.ca (E.K. Skierszkan).

http://dx.doi.org/10.1016/j.scitotenv.2016.01.053
0048-9697/

1. Introduction

Leaching of metals during sulfide oxidation reactions in mining waste rock dumps presents a global environmental challenge, the mitigation of which requires a detailed understanding of the geochemical behavior of metals in these systems. Molybdenum (Mo) and zinc (Zn) are two metals which can be released at elevated concentrations during weathering of sulfidic waste rock (e.g. Kaback, 1976; Sahu et al., 1994). Both of these elements are important micronutrients, but can cause toxic effects at elevated environmental concentrations: excess Mo is particularly harmful to ruminants which are susceptible to molybdenosis (Barceloux, 1999) and Zn toxicity has been reported in plants, humans, cattle, and invertebrates (Canadian Council of Ministers of the Environment, 1999; Valko et al., 2005).

Molybdenum and zinc are released from mine wastes during the oxidative weathering of the sulfide ore minerals molybdenite (MoS_2) and sphalerite (ZnS), respectively:

$$2MoS_2 + 9O_2 + 6H_2O \rightarrow 2MoO_4^{2-} + 4SO_4^{2-} + 12H^+ \quad (1)$$

$$ZnS + 2O_2 \rightarrow Zn^{2+} + SO_4^{2-}. \quad (2)$$

Because aqueous Mo forms an anionic molybdate species (MoO_4^{2-}) while Zn forms a weakly-hydrolyzing cation (Zn^{2+}), the response of these metals to changes in pH in mine drainage is distinct (Dockrey and Stockwell, 2012) and their mobility may be reduced by different attenuation processes (e.g. adsorption, secondary mineral formation). Molybdate (MoO_4^{2-}) is strongly adsorbed onto oxyhydroxide minerals in moderately acidic conditions (Goldberg et al., 1996; Gustafsson, 2003; Xu et al., 2006), but is mobile in neutral to alkaline pH conditions where its adsorption is minimal. In alkaline mine drainage, molybdate minerals powellite ($CaMoO_4$) and wulfenite ($PbMoO_4$) can act as Mo solubility controls (Conlan et al., 2012). In contrast, Zn exhibits an opposite response to pH relative to Mo: it is mobilized in acidic conditions while attenuation processes reduce its mobility in alkaline conditions. Attenuation mechanisms for Zn in mine drainage include adsorption onto oxyhydroxide and carbonate minerals (Gupta et al., 1987; Iavazzo et al., 2012; Laurenzi et al., 2015), and the formation of a variety of secondary minerals such as $Zn(OH)_2$, carbonates (e.g. smithsonite ($ZnCO_3$), hydrozincite ($Zn_5(OH)_6(CO_3)_2$), silicates (e.g. willemite Zn_2SiO_4, hemimorphite $Zn_4Si_2O_7(OH)_2 \cdot H_2O$) and sulfates (e.g. zincosite, $ZnSO_4$) (Hirsche, 2012; Iavazzo et al., 2012; Jacquat et al., 2008; Wanty et al., 2013a, 2013b).

Conventional geochemical and mineralogical investigations have yielded some insights into which processes are responsible for metal attenuation in mining waste rock dumps. However, uncertainty remains with regard to the long-term fate of metals in mine wastes, in large part due to the difficulty in accessing the interior of dumps for sampling, and also due to the inherent mineralogical and hydrological heterogeneity of waste rock (Amos et al., 2015). Recent analytical improvements in mass spectrometry now permit the accurate and precise measurement of small variations in metal isotope ratios, which have been increasingly utilized as tracers of metal attenuation processes in the environment (Wiederhold, 2015). Metal isotope ratios may therefore become useful monitoring parameters for the characterization of mine drainage effluent (Matthies, 2015) by recording the geochemical history of attenuation processes which occur within waste rock dumps, provided these processes impart distinct isotopic signatures on the residual dissolved metal pool.

A small number of studies have investigated the applicability of Zn isotopes as tracers of Zn geochemistry in mine drainage. Matthies et al. (2014b) monitored Zn isotopic compositions of moderately acidic (pH ~4–6.5) mine drainage in an experimental waste rock pile and found small variations in δ^{66}Zn which averaged $+0.06 \pm 0.08$‰ (2 SD, n = 43) relative to the IRMM 3702 Zn isotope standard over a 2-year monitoring period, suggesting little effect of secondary processes on Zn isotope ratios in waste rock drainage under those conditions. However, a subsequent study found a range in δ^{66}Zn of 0.4‰ during experimental leaching of sulfidic mine tailings, which was hypothesized to be caused by release of Zn from distinct mineral phases bearing different isotopic compositions (Matthies et al., 2014a). Other studies have examined Zn isotope compositions in surface waters downstream of historical acid-rock drainage (ARD) sites where limited variations in δ^{66}Zn were found, which led to the proposition that Zn stable isotope ratios were more likely to be tracers of Zn sources rather than attenuation processes, due to its conservative isotopic and geochemical behavior in such conditions (Aranda et al., 2012; Borrok et al., 2008; Fernandez and Borrok, 2009). All of these studies pointed to a relatively narrow range in δ^{66}Zn in ARD. No studies so far have expanded analyses to directly include alkaline pH mine drainage where Zn attenuation processes including adsorption and secondary Zn carbonate and hydroxide mineral formation are of greater importance. However, studies by Wanty et al. (2013a, 2013b) in an alkaline-pH river (pH ~8) with an elevated dissolved Zn load from mining activities showed that Zn was removed during precipitation of hydrozincite and amorphous Zn-silicate minerals which had δ^{66}Zn values that were 0.35 to 0.5‰ heavier compared to the dissolved Zn load. Laboratory experiments have also confirmed that hydrozincite precipitation removes heavy Zn isotopes from solution (Veeramani et al., 2015).

There have been no studies of Mo isotope compositions in waste rock drainage to date. However, a compilation of natural and experimental samples measured thus far showed a substantial degree of fractionation in δ^{98}Mo exceeding 6‰ (Goldberg et al., 2013). Mo adsorption is known to drive changes in Mo isotope ratios in solution: Fractionation factors for Mo adsorption ($\alpha_{solution\text{-}adsorbed}$) range from 1.00083 to 1.00276 depending on the adsorbent mineral (Barling and Anbar, 2004; Goldberg et al., 2009; Wasylenki et al., 2008). Molybdate (MoO_4^{2-}) conversion to thiomolybdate ($MoO_xS_{4-x}^{2-}$) in sulfidic waters can also drive a preferential removal of light Mo isotopes from solution (Nägler et al., 2011), although this Mo removal pathway is not expected in oxidized waste rock drainage where sulfur speciation is dominated by SO_4^{2-}.

These previous studies of Mo and Zn indicate that their isotopic variation may be useful parameter to track the geochemical fate of these metals in waste rock drainage. However, more measurements of δ^{66}Zn are necessary to constrain our understanding of its isotopic behavior in waste rock drainage, in particular in alkaline-pH mine drainage where Zn attenuation is stronger. In addition, δ^{98}Mo has yet to be explored as a tracer of Mo in mine wastes. Therefore, the objectives of the present study were twofold: (1) to evaluate the extent of isotopic variability of Mo and Zn source minerals at a mine site with lithological heterogeneity in its waste rock, and (2) to evaluate whether isotopic fractionation in mine drainage was occurring after release of Mo and Zn to solution via sulfide mineral oxidation. The Mo and Zn isotopic compositions of source minerals were characterized by analyzing solid phase samples that included waste rock, ore minerals collected from drill core, and ore concentrate. The role of secondary processes on Mo and Zn isotopic compositions in mine drainage was investigated by analyzing water samples from small- to intermediate-scale waste rock weathering experiments under field conditions covering a range in pH from acidic to alkaline. Samples were collected at the Antamina Cu–Zn–Mo–(Pb–Ag–Bi) mine, Peru, where multi-scale weathering experiments are under way to assess metal release and transport processes in mining waste rock dumps.

2. Study site

The Antamina deposit is a polymetallic skarn emplaced during a mid-Cenozoic quartz monzonite porphyry intrusion into Late Cretaceous limestone (Lipten and Smith, 2004). It is located at high elevation (4100–4700 m) in the Peruvian Andes (9° 32 S, 77° 03 W) (Fig. 1). The average annual temperature is between 5.5 and 6.0 °C, and annual

precipitation is 1200–1300 mm, of which the vast majority (80–90%) falls during a distinct rainy season typically lasting from October to April (Blackmore et al., 2014).

The geology of the deposit is described in detail in Beckie et al. (2011) and Lipten and Smith (2004). A sequence of overlapping intrusions and metasomatic processes into the original carbonate terrain produced a highly heterogeneous deposit, which is also reflected in the waste rock. Major rock types can broadly be grouped into quartz monzonite intrusive, endoskarn, exoskarn, marble, hornfels and limestone, although further subdivisions exist within these groups.

Field weathering experiments were initiated in 2005 at Antamina to identify hydrological and geochemical processes in waste rock at different scales. In particular, this investigation includes the implementation of small-scale "field barrel" and intermediate-scale "constructed pile" experiments (Beckie et al., 2011). Field barrels are ~1 m high rain barrels filled with ~350 kg of a specific waste rock type (Supplementary Fig. S1a). Constructed pile experiments consist of 36 m long × 36 m wide × 10 m high piles of waste rock containing ~25,000 t of material of specific lithologies that were constructed by end-dumping waste rock with haul trucks (Supplementary Fig. S1b). Both field barrels and piles are subjected to weathering under field conditions and their drainage hydrogeochemistry is routinely monitored. Further details of the construction and instrumentation of the field barrels and piles can be found in Bay (2009); Corazao Gallegos (2007), and Aranda (2010).

Quantitative mineralogy of the waste rock emplaced in field barrel and constructed pile experiments has been characterized previously using powder X-ray diffraction (XRD) with Rietveld Refinement (Dockrey, 2010; Peterson, 2014). Waste rock lithologies in this study (intrusive, endoskarn, exoskarn, marble and hornfels) contain variable sulfide amounts, ranging 0.2 to 15 wt.% (Table S1, supplementary information). Molybdenite abundance is greatest in endoskarn and intrusive waste rock, where it is present at concentrations close to the detection limit of XRD (~0.5 wt.%), and sphalerite is mainly enriched in exoskarn waste rock (0.4–5.1 wt.%). Both molybdenite and sphalerite are also present at low-concentrations in other waste rock types, as detectable using scanning-electron microscopy coupled with mineral liberation analysis software (SEM-MLA) (Aranda, 2010). Other sulfide minerals include chalcopyrite, pyrite, pyroaurite and pyrrhotite. Calcite is present (2–87 wt.%) in all lithologies except intrusive waste rock, and provides acid-buffering capacity in those materials.

Fig. 1. Location of the Antamina Mine, Peru.

3. Methods

3.1. Sample selection and preparation

An array of solid phase samples was collected to assess the source isotopic variability for Mo and Zn in Antamina molybdenites, sphalerites and waste rock. Unweathered ore-grade molybdenite and sphalerite samples were subsampled from Antamina drill-core from a range of mineralized areas from within the deposit. For molybdenites, individual grains weighing a few mg each were hand-picked from drill-core samples and dissolved in Savillex® beakers on a hot-plate in 3 mL of a 3:1 mixture of concentrated HCl and HNO_3 and then re-constituted in ~30 mL of 5 vol.% HNO_3–1 vol.% HF for storage and mass spectrometric analysis. For sphalerites, drill-core hand samples containing 12–40% Zn (as indicated by chemical assays done by mine geologists) were pulverized using a ring-mill. Depending on zinc concentrations, 1–14 mg aliquots of the powdered sphalerite ores were weighed into Savillex® beakers and dissolved in 0.75 mL of 2:1 concentrated HNO_3 and HCl on a hotplate for ~60 h. The sphalerite samples were then evaporated and re-constituted in 2 mL of concentrated HCl. They were centrifuged to remove any residual refractory minerals which were discarded while the supernatant containing the dissolved sphalerites was retained for mass spectrometry.

A sample of molybdenite ore concentrate was also obtained from the mine. Molybdenum ore at Antamina is processed on site, beginning with a primary crusher followed by further grinding using a Semi-Autogenous Grinder (SAG) mill. After milling, ore is further pulverized by a series of ball-mills and then sulfides are extracted from host rock using hydrochemical flotation (Bay, 2009). Approximately 40 mg of molybdenite ore concentrate containing ~50 wt.% Mo was dissolved in 8 mL of 3:1 HCl:HNO_3 on the hotplate. Three successive treatments of this mixture were required for full dissolution of the ore, after which it was evaporated and re-constituted in 5% (vol.) HNO_3 – 1% (vol.) HF for storage prior to analysis.

Waste rock samples included exoskarn material from field barrel UBC-3-1A and intrusive material from field barrel UBC-2-3A. The exoskarn waste rock sample was collected prior to the beginning of field barrel experiment and stored dry to avoid any weathering effects. The intrusive waste rock sample was collected directly from the field barrel and therefore had been exposed to weathering. In order to minimize secondary weathering effects in the intrusive waste rock, a large cobble-sized sample showing little surface alteration was selected. Waste rock samples were pulverized using a ring mill and aliquots of rock powders were weighed into Savillex® beakers for total hotplate acid digestion. Because of the elevated carbonate and silicate content of Antamina waste rock, the multi-stage dissolution method of Connelly et al. (2006) was used, in which silicates are dissolved in a mixture of HF-HNO_3 followed by treatment with a mixture of HNO_3-H_3BO_3 to remove any insoluble fluoride precipitates by complexation of B and F^-. All acids used in the digestion of solid phase samples were purified in-house from concentrated reagent grade acids by sub-boiling distillation, and sample dissolution was conducted in metal-free Class 1000 clean laboratories at the Pacific Centre for Isotopic and Geochemical Research (PCIGR), University of British Columbia (Vancouver, Canada).

Waste rock drainage samples were collected from field barrels and experimental waste rock piles at Antamina during three sampling trips to the mine between November 2012 and April 2014. Samples were selected to represent drainage from a variety of waste rock lithologies present at Antamina, in both the barrel- and the pile-scales.

This included field barrels and piles containing intrusive, exoskarn, endoskarn, marble and hornfels waste rock encompassing drainage pH values ranging from <3 to >8. Samples were filtered in the field using 0.2 μm filters or, if unavailable, 0.45 μm filters, and preserved with reagent-grade HNO_3 to pH <2 prior to shipment to the laboratory. Field-filtered blanks for Mo and Zn were regularly monitored to ensure no contamination occurred during the sampling and preservation process. In the clean laboratory, aliquots of water samples were reconstituted in dilute (1 vol.% HNO_3 0.05 vol.% HF) acid solutions for elemental analysis by ICP-MS (Agilent 7700×, Agilent Technologies, Santa Clara, CA, USA) at PCIGR.

3.2. Analytical

Elemental concentrations for solid phase and aqueous samples were determined by ICP-MS (Agilent 7700×) using an external multi-element calibration standard and indium as an internal drift correction standard. Prior to isotopic analysis, Mo and Zn fractions were isolated from the sample matrices using the ion-exchange purification scheme of Skierszkan et al. (2015): Briefly, samples were dissolved in 7 N HCl and loaded onto 2 mL of BioRad AG® MP-1 M resin (100–200 mesh). Most matrix elements are removed in 7 N HCl and 4 N HCl, after which successive elutions of Fe (1 N HCl 0.5 N HF), Mo (2 N HCl 8 N HF) and Zn (0.1 N HBr 0.5 N HNO_3) are possible. Replicate trials of synthetic multi-element solutions and USGS basalt BCR-2 show recoveries of 94–97% for Mo and 100–103% for Zn using this purification scheme.

Molybdenum isotopic compositions on the pure sample fractions were measured using a Nu Plasma MC-ICP-MS (Nu 21, Nu Instruments Ltd., Wrexham UK). A ^{97}Mo–^{100}Mo double-spike was used to correct for laboratory and instrumental mass fractionation using the method presented in Skierszkan et al. (2015). The Mo double-spike was added prior to ion-exchange purification to account for any possible Mo isotopic fractionation on the ion-exchange column. After ion-exchange purification, samples were re-constituted in 2 vol.% HNO_3 0.1 vol.% HF and introduced into the plasma using a DSN-100 desolvating nebulizer (Nu Instruments Ltd., Wrexham UK). Molybdenum isotope masses 92–100 were monitored in static mode using 30 measurement cycles each having a 10 s integration time and a 2 s magnet settling time. On-peak zero blanks and ESA deflection blanks were measured and subtracted from raw sample isotope intensities. For each batch of samples, accuracy was monitored by analyzing a reference material (e.g., BCR-2, SDO-1 or open ocean water) along with samples through the full ion-exchange and analytical procedure. Molybdenum isotope compositions are reported using the $\delta^{98}Mo$ notation:

$$\delta^{98}Mo_{sample}\ (‰) = \left(\frac{\left(\frac{^{98}Mo}{^{95}Mo}\right)_{sample}}{\left(\frac{^{98}Mo}{^{95}Mo}\right)_{standard}} - 1 \right) \times 1000. \quad (3)$$

All $\delta^{98}Mo$ data presented in this study follow the convention recommended by Nägler et al. (2014), i.e., sample Mo isotope ratios are normalized to NIST-SRM-3134 = +0.25‰. Using this notation, our in-house Mo isotope standard "Mo(UBC)", defined in Skierszkan et al. (2015), has a $\delta^{98}Mo$ value of 0.07‰ relative to the NIST-SRM-3134 = +0.25‰. The long-term running average 2 SD reproducibility for analyses of Mo (UBC) is 0.05‰ (n = 165).

Zinc isotope measurements of pure sample fractions were also conducted on the Nu Plasma MC-ICP-MS, using the operational settings and methods presented in Shiel et al. (2013) and Shiel et al. (2009). For Zn isotopic analysis, samples and standards were doped with a pure Cu solution (High Purity Standards, Charleston, SC, USA lot 510,232) in a 3:1 Cu:Zn ratio (based on mass concentrations) and were introduced into the instrument in wet plasma mode. Mass bias corrections were done using a combination of standard-sample-bracketing and exponential law normalization (e.g. Maréchal et al. (1999)) of the $^{66}Zn/^{64}Zn$ ratio using $^{65}Cu/^{63}Cu$. Online corrections of possible interferences of ^{64}Ni on ^{64}Zn were achieved by monitoring ^{62}Ni. All sample measurements were done in triplicate, and prior to sample analysis, instrumental accuracy was monitored by measuring a secondary Zn isotope standard (PCIGR-2 Zn, which is 10.38 ± 0.12‰ (2 SD, n = 40) lighter than our primary in-house standard (PCIGR-1 Zn) as defined in Shiel et al. (2009). Three isotope plots of $\delta^{68/64}Zn$ as a function of $\delta^{66/64}Zn$ showed that samples were free from isobaric interferences and displayed mass-dependent fractionations (Supplementary Fig. S2). Zn isotope ratios were expressed using the $\delta^{66}Zn$ ratio as follows:

$$\delta^{66}Zn_{sample}\ (‰) = \left(\frac{\left(\frac{^{66}Zn}{^{64}Zn}\right)_{sample}}{\left(\frac{^{66}Zn}{^{64}Zn}\right)_{PCIGR-1\ Zn)}} - 1 \right) \times 1000. \quad (4)$$

Repeated measurements of the PCIGR-1 Zn reference standard in wet plasma on two Nu Plasma MC-ICP-MS instruments (Nu21, NP214) at PCIGR show that it is 0.11 ± 0.05‰ (2 SD, n = 8) heavier than the commonly used Zn isotope standard of the École Normale Supérieure de Lyon's Earth Science Laboratory, "JMC-Lyon" (JMC Zn standard solution, batch 3–0749 L). For each batch of sample analyses in this study, an aliquot of PCIGR-1 Zn was also passed through ion-exchange purification and analyzed on the MC-ICP-MS for quality control. Concentrations of samples and bracketing standards were generally similar within <10% and always <25%. A test of our secondary standard (PCIGR-2 Zn) showed that $\delta^{66}Zn$ measurements remained accurate within a deviation in concentration of 30% between the bracketing standards and the sample.

In addition to the water samples which were collected from field barrels and experimental waste rock piles for isotopic analysis, weekly or monthly water sampling was routinely conducted at the mine and samples were analyzed for full routine geochemical parameters (pH, alkalinity, major and minor cations and anions). These data were used to calculate mineral saturation indices (SI) to identify possible mineral solubility controls on Mo and Zn. This analysis was extended to cover the entire rainy season during which isotope sampling events occurred to give a general understanding of saturation states of likely Mo and Zn secondary minerals in each field barrel and waste rock pile. Mineral SI calculations were computed using the PHREEQC code (Parkhurst and Appelo, 2013) with the WATEQ4F mineral database. Chemical reactions and mineral solubility constants involving Mo aqueous species and minerals (powellite, wulfenite) were added to the WATEQ4F database as described in Conlan et al. (2012). In addition, we included hydrozincite data in the WATEQ4F database, using the solubility constant determined by Preis and Gamsjäger (2001).

4. Results and discussion

4.1. Molybdenum isotope composition of waste rock, ores and mine drainage

Molybdenum isotopic compositions in all solid phase samples exhibited significant heterogeneity with a range in $\delta^{98}Mo$ spanning 1.2‰ (Table 1), and overlap in $\delta^{98}Mo$ between endoskarn-hosted and intrusive-hosted molybdenite (Fig. 2). These results follow a growing body of research demonstrating large Mo isotope fractionation in molybdenites, which are thought to be related to high-temperature Mo redox changes during ore genesis or Rayleigh-type distillation during the precipitation of molybdenite from hydrothermal vapors (Greber et al., 2014, 2011; Hannah et al., 2007; Mathur et al., 2010; Wieser and de Laeter, 2003; Yang et al., 2015). While the scale of spatial variability in molybdenite isotope compositions was not systematically evaluated in this study, others have shown that Mo isotope fractionation can occur within hand-samples and single crystals (Hannah et al., 2007; Mathur et al., 2010). Evidence for Mo isotopic heterogeneity

Table 1
Molybdenum isotopic compositions of mine drainage, molybdenites, waste rock and ore concentrate from the Antamina mine.

Sample ID	Lithological association	Mo	pH	2 SD[b]
		ppm	δ^{98}Mo[a]	‰
Mine drainage samples				
Field barrels				
Celda-07-14	Endoskarn	11.5	7.2	−0.06 ± 0.05
Celda-07-13	Endoskarn	13.9	8.2	−0.15 ± 0.02
UBC-2-0A	Intrusive	0.62	7.9	0.45 ± 0.05
UBC-2-1A	Intrusive	1.69	8.4	0.33 ± 0.02
UBC-2-3A	Intrusive	0.16	2.2	0.68 ± 0.03
UBC-5-2A	Intrusive	0.65	8.0	1.31 ± 0.04
UBC-3-1A-14	Exoskarn	0.19	7.2	1.35 ± 0.06
UBC-3-1A-13	Exoskarn	0.27	7.6	1.35 ± 0.03
UBC-5-0A	Hornfels	0.02	7.9	0.89 ± 0.07
UBC-3-3A	Exoskarn	0.015	7.8	0.73 ± 0.04
UBC-4-4A	Marble	0.010	8.6	2.07 ± 0.04
UBC-4-5-1A	Hornfels	0.010	8.1	0.48 ± 0.04
Experimental waste rock piles				
UBC-2-D-12	Intrusive	4.69	6.1	1.17 ± 0.02
UBC-2-D-14	Intrusive	0.50	2.9	1.30 ± 0.04
UBC-3-D	Exoskarn	0.013	7.5	1.76 ± 0.01
UBC-5-D	Intrusive with hornfels	0.91	7.9	0.50 ± 0.04
Solid-phase samples				
Molybdenites				
A1392	Endoskarn	–		0.18 ± 0.07
A2793d	Endoskarn	–		−0.21 ± 0.05
A813	Endoskarn	–		0.61 ± 0.10
A2062	Endoskarn	–		0.57 ± 0.04
A813	Endoskarn	–		0.55 ± 0.06
C-07_MoS2C-07_MoS2	Endoskarn	–		0.09 ± 0.04
2-3A_MoS22-3A_MoS2	Intrusive	–		0.22 ± 0.05
A1363	Intrusive	–		−0.55 ± 0.04
A2194	Intrusive	–		−0.28 ± 0.04
Ore concentrate				
Mo2496	N/A	–		0.11 ± 0.07
Waste rock				
UBC-2-3A_WR	Intrusive	626		0.47 ± 0.05
UBC-3-1A_WR	Exoskarn	82		0.47 ± 0.03

[a] δ^{98}Mo expressed relative to NIST-SRM-3134 = +0.25‰.
[b] 2 SD for triplicate analysis on the MC-ICP-MS.

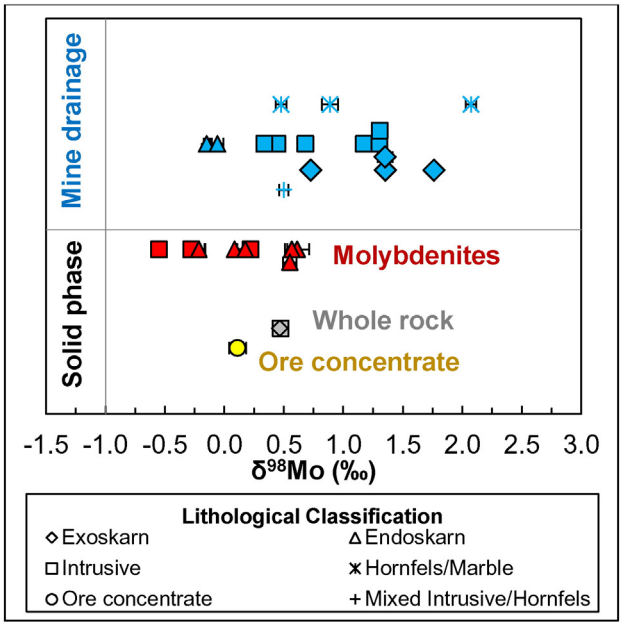

Fig. 2. Molybdenum isotopic compositions of mine drainage from experimental field barrels and waste rock piles, and of molybdenites, waste rock and ore concentrate. Data are spread vertically for clarity. δ^{98}Mo is reported relative to NIST-SRM-3134 = +0.25‰. Error bars are 2 SD for triplicate analysis on the MC-ICP-MS, and are typically smaller than symbol size.

at small scales was also seen in Antamina mine wastes: a powdered whole-rock analysis of intrusive waste rock and a single molybdenite grain picked from the same material prior to crushing differed by 0.2‰ in δ^{98}Mo (samples UBC-2-3A_WR and 2-3A_MoS$_2$, Table 1).

Although the occurrence of such isotopic variations in molybdenite at small scales presents a challenge to define the isotopic composition of the source of Mo in waste rock drainage, at larger scales (i.e. waste rock dumps) the input δ^{98}Mo signature to mine drainage should reflect a deposit-scale averaged isotopic composition of molybdenites, thereby reducing the effect of these small-scale variations. Our best estimate for this averaged source value at Antamina is provided by the Mo isotopic composition of MoS_2 ore concentrate, which is produced by milling and blending molybdenite ore and isolating it through hydrochemical flotation. The ore concentrate's isotopic composition of 0.11 ± 0.07‰ (2 SD) should therefore reflect a δ^{98}Mo composition averaged over larger scales within pit domains. No isotopic fractionation is anticipated as a result of ore processing at the mine because MoS_2 is concentrated by density separation that does not involve breaking of Mo-S bonds. The ore concentrate isotopic composition compared favorably to an average δ^{98}Mo of 0.13 ± 0.82‰ (2 SD, n = 9) for all the Antamina molybdenites analyzed in this study (Fig. 2). Upper and lower bounds defined by the range of δ^{98}Mo found in molybdenites are −0.55 to +0.61‰.

Large variations of δ^{98}Mo spanning 2.2‰ were found in samples of mine drainage collected from field barrels and experimental waste rock dumps weathering under field conditions. The range isotopic composition for mine drainage was −0.15 to +2.07‰ (Table 1) and the average δ^{98}Mo was heavier (0.89‰ ± 1.25, 2 SD, n = 16) relative to the solid phase, which indicated that Mo isotopic fractionation arose either during oxidative MoS_2 dissolution or during subsequent aqueous reactions (Fig. 2). There was no clear association of waste rock lithology and δ^{98}Mo in drainage waters as water samples originating from different waste rock types exhibited some overlap in Mo isotope ratios (Fig. 2).

The shift to heavier δ^{98}Mo in mine drainage samples relative to the range observed in the solid phase (Fig. 2) is consistent with observations of heavier Mo isotope signatures in solutions relative to rocks and minerals at a global scale. The average δ^{98}Mo of the continental crust is estimated at 0.3–0.4‰ (Greber et al., 2014, 2015), in comparison to an average value of 0.89 ± 0.91‰ (2 SD, n = 65) for rivers (Archer and Vance, 2008; Neubert et al., 2011; Voegelin et al., 2012) and 2.3‰ for the ocean (Nakagawa et al., 2012). Any combination of three possible hypotheses can explain the heavy δ^{98}Mo signature of mine drainage samples: (1) δ^{98}Mo in mine drainage reflects heterogeneity in the source δ^{98}Mo signature (i.e. molybdenites); (2) oxidative molybdenite dissolution results in the preferential release of heavy Mo isotopes; and (3) there is retention of light Mo isotopes during Mo attenuation processes such as adsorption or formation of secondary molybdate minerals (e.g. powellite, wulfenite).

Although some degree of heterogeneity in solid-phase Mo isotopic compositions was found, it is improbable that source isotopic compositions can fully explain the shift towards heavier δ^{98}Mo values measured in mine drainage samples (Fig. 2). The heaviest δ^{98}Mo measured in our array of solid phase samples was 0.6‰ (molybdenite A813), which constitutes an upper bound for the solid phase Mo isotopic compositions. In contrast, ten of the sixteen measurements of δ^{98}Mo in drainage waters were heavier than this 0.6‰ upper bound value for solid phase δ^{98}Mo. In addition, δ^{98}Mo values in mine drainage coming from the two field barrels for which whole-rock δ^{98}Mo measurements were available (UBC-2-3A and UBC-3-1A) also showed shifts towards heavier isotopic compositions in solution: $\Delta^{98}Mo_{solution\text{-}whole\ rock}$ values (defined as $\Delta^{98}Mo_{solution\text{-}whole\ rock} = \delta^{98}Mo_{solution} - \delta^{98}Mo_{whole\ rock}$)

were +0.21 and +0.88‰, respectively. Calculating an average isotopic separation factor as $\Delta^{98}Mo_{solution\text{-}solid}$ ($\Delta^{98}Mo_{solution\text{-}solid} = \delta^{98}Mo_{solution} - \delta^{98}Mo_{ore\ concentrate}$) between mine drainage and the ore concentrates used as a proxy for the average molybdenite δ^{98}Mo value for all water samples give a $\Delta^{98}Mo_{solution\text{-}solid}$ value of +0.77 ± 1.25‰ (2 SD, n = 16). These observations indicate that the shift towards heavier isotopic compositions in drainage water cannot solely be attributed to variability in the solid phase signature.

A second hypothesis to explain the shift towards heavier δ^{98}Mo in solution is that molybdenite dissolution preferentially releases heavy Mo isotopes to solution due to a change in bonding environment between trigonal-prismatic $Mo^{IV}S_2$ and tetrahedral $Mo^{VI}O_4^{2-}$ (Johansson and Caminiti, 1986; Ramana et al., 2008). At present the exact mechanism of isotopic fractionation during mineral dissolution reactions is poorly understood due to the complexity and possible co-mingling of various processes during dissolution, such as the limited availability of atoms at the mineral surface for dissolution reactions, the role of interactions between ligands in solution and atoms at the mineral surface, microbial processes, mineralogical heterogeneity and overlapping kinetic and equilibrium isotope effects (Wiederhold, 2015). These complications make it difficult to predict *a priori* the direction and magnitude of any Mo isotopic fractionation during mineral dissolution. Empirical observations of the preferential release of heavy Mo isotopes during Mo dissolution experiments were found in studies by Liermann et al. (2011) and Voegelin et al. (2012), while Siebert et al. (2003) observed no fractionation during leaching. However, the ~0.3‰ enrichment in heavy Mo isotopes observed by Liermann et al. (2011) during dissolution of Mo-rich shale was interpreted to be driven by secondary adsorption onto Fe-Mn oxyhydroxides rather than fractionation during the leaching process itself. Meanwhile, Voegelin et al. (2012) attributed 0.5–1.1‰ enrichments in δ^{98}Mo during leaching of igneous rocks to the preferential release of a sulfide-bound Mo pool which was isotopically heavier than the silicate matrix and the bulk rock. This interpretation is supported by the observation that heavy Mo isotopes preferentially accumulate in Mo-sulfide phases and in molybdenites rather than the silicate melt in high-temperature Mo ore genesis processes (Greber et al., 2014). In the context of weathering of molybdenite-rich waste rock, molybdenite rather than silicate-bound Mo will dominate the pool of labile Mo. As discussed above, the average isotopic composition of Antamina molybdenite is not expected to exceed 0.6‰ and is more likely close to the ~0.1‰ value of the MoS_2 ore concentrate. We therefore conclude that secondary processes occurring after oxidative MoS_2 dissolution were most likely responsible for driving the shift towards heavier δ^{98}Mo signatures observed in mine drainage relative to molybdenites, rather than the molybdenite dissolution process.

Molybdenum adsorption is known to preferentially remove light Mo isotopes with fractionation factors ($\alpha_{solid\text{-}solution}$) in the range of 1.00083–1.00276 (Barling and Anbar, 2004; Goldberg et al., 2009; Wasylenki et al., 2008). Adsorption can be anticipated in weathered waste rock, where accelerated pyrite and silicate weathering leads to an abundance of Fe, Mn and Al oxyhydroxide minerals that can act as adsorbents. Adsorption is strongest for Mo at a moderately acidic pH range of 4–5 and is reduced in alkaline pH conditions (Goldberg et al., 1996; Gustafsson, 2003; Xu et al., 2006). Most mine drainage samples had neutral to alkaline pH, where Mo adsorption onto oxyhydroxide minerals is anticipated to be small, yet, surprisingly, among samples with pH > 7, the full range in δ^{98}Mo spanning 2.2‰ was observed (Fig. 3). However, acidic micro-sites have been shown to occur in weathered Antamina waste rock that releases bulk neutral-pH drainage (Dockrey et al., 2014). It is therefore plausible that localized Mo adsorption in acidic micro-sites is responsible for retaining light Mo isotopes from solutions that display bulk neutral-pH, and drives the shift towards heavier δ^{98}Mo values in mine drainage. Evidence for adsorbed Mo was found in chemical sequential extractions of weathered Antamina waste rock conducted by Laurenzi et al. (2015) where Mo was leached during the dissolution of crystalline reducible phases corresponding to iron oxides (Hall et al., 1996). It is therefore likely that Mo adsorption is occurring in Antamina waste rock and driving the shift towards heavier δ^{98}Mo in mine drainage.

In addition to considering the role of adsorption, secondary minerals, including powellite ($CaMoO_4$) and wulfenite ($PbMoO_4$), are known to attenuate Mo in mine wastes and have been observed at Antamina (Conlan et al., 2012). The isotopic fractionation associated with their formation is not known. However, the chemical environment for Mo in both powellite and wulfenite is similar to aqueous molybdate anions, characterized by tetrahedrally-coordinated Mo atoms bonding with oxygen atoms at interatomic distances of 1.76–1.77 Å (Achary et al., 2006; Cora et al., 2011; Johansson and Caminiti, 1986; Lugli et al., 1999). The lack of differences in Mo bonding and coordination in aqueous molybdate and metal molybdate minerals leads to the *a priori* hypothesis that any equilibrium Mo isotope fractionation should be minimal during mineral precipitation (Schauble, 2004), although this should be tested empirically. If Mo removal during molybdate mineral precipitation is a kinetic, rather than equilibrium process, isotope fractionation favoring removal of lighter Mo isotopes would be expected.

Powellite mineral saturation indices (SI) at the field barrel scale were consistently <0 throughout the study period in all field barrels (Fig. 4) except Celda-07, which had significantly higher aqueous Mo concentrations (Table 1). With the exception of Celda-07, powellite precipitation was therefore not expected to play a major role at the field

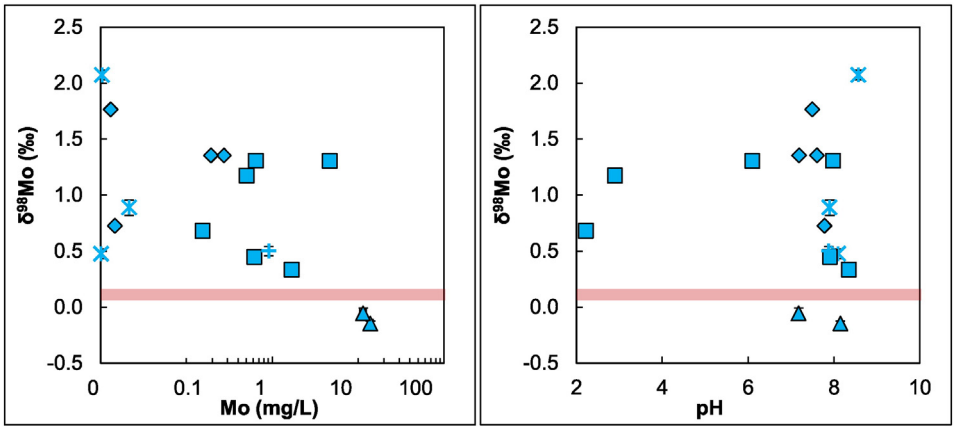

Fig. 3. Molybdenum isotope compositions in mine drainage collected from experimental field barrels and waste rock piles, plotted against molybdenum concentrations (left) and pH (right). Symbol shape indicates lithology in field barrel or pile, as in Fig. 2. Horizontal shadow shows the isotopic composition of Antamina molybdenite ore concentrate. Error bars are 2 SD for triplicate analysis on the MC-ICP-MS and are typically smaller than measurement symbol.

barrel scale and should have had little impact on dissolved Mo isotope compositions (Fig. 4). In the case of field barrel Celda-07, powellite formation was favored by high molybdenite contents in that material (0.2 wt.%, Table S1) and alkaline pH (7.2–8.2 during this study period, Table 2) which leads to dissolved Mo concentrations that are 1–2 orders of magnitude higher than in all of the other field barrels (Table 2). The occurrence of powellite in Celda-07 has also been confirmed by SEM-MLA (Fig. 12 c) and d) in Conlan et al., 2012). However, we consider that powellite formation in Celda-07 is unlikely to have caused significant Mo isotope fractionation in drainage from that field barrel. As mentioned previously, equilibrium isotope fractionation associated with powellite formation should be negligible due to similar Mo bonding environments in aqueous MoO_4^{2-} and in powellite (Achary et al., 2006; Johansson and Caminiti, 1986). In addition, if significant kinetic isotope fractionation were occurring during powellite formation in Celda-07, we would expect a shift towards heavier δ^{98}Mo in the residual aqueous Mo pool. However, Celda-07's dissolved Mo isotope composition was the lightest among all mine-drainage samples. Furthermore, given the exceptionally high Mo concentrations released from this field barrel, mass balance would require that a very high proportion of Mo would have had to be removed by secondary processes to cause any measurable isotope effect in the remaining solution, which is unlikely given the slow reaction kinetics of powellite formation (Conlan et al., 2012). We therefore conclude that the relatively light δ^{98}Mo value of mine drainage in Celda-07 likely reflected direct dissolution of molybdenite with limited effect of secondary processes.

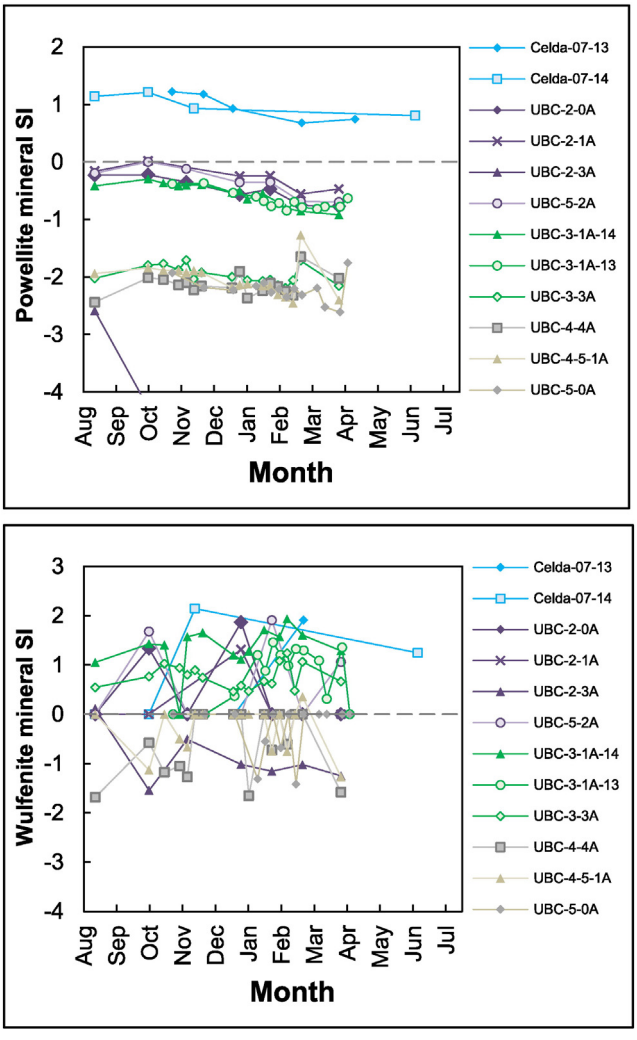

Fig. 4. Seasonal variation in powellite (top) and wulfenite (bottom) mineral saturation indices (SI) in field barrel drainage calculated using PHREEQC. Data are shown for the entire rainy season during which a sample was drawn for Mo isotope analysis. Isotope sampling was conducted in April. Wulfenite data series are discontinuous when dissolved Pb concentrations were not measured above the detection limit by ICP-MS. Note differences in y-axis scales. Also note that UBC-2-3A mineral SIs for powellite were typically lower than the range shown on the y-axis in the figure. Horizontal dashed line indicates SI = 0.

Table 2
Zinc isotopic compositions of mine drainage, sphalerites and waste rock from the Antamina mine.

Sample ID	Lithological association	Zn	pH	δ^{66}Zn[a] ± 2 SD[b]
		ppm		‰
Water samples				
Field barrels				
UBC-2-0A	Intrusive	1.1	7.9	0.03 ± 0.05
UBC-2-3A	Intrusive	7.8	2.2	0.30 ± 0.03
UBC-3-1A-14	Exoskarn	2.3	7.2	−0.06 ± 0.07
UBC-3-1A-13	Exoskarn	2.8	7.6	−0.02 ± 0.05
UBC-3-2A	Exoskarn	15.6	7.8	−0.17 ± 0.11
UBC-3-3A	Exoskarn	0.3	7.8	−0.35 ± 0.07
UBC-4-4A	Hornfels	0.2	8.6	−0.17 ± 0.02
Experimental waste rock piles				
UBC-2-D-14	Intrusive	667	2.9	0.15 ± 0.05
UBC-2-D-12	Intrusive	135	6.1	0.07 ± 0.04
UBC-3-D	Exoskarn	11.8	7.5	−0.03 ± 0.12
UBC-5-D	Intrusive and hornfels	0.2	7.9	−0.01 ± 0.05
Solid phase				
A1463	Ore-grade sphalerite	152,316		0.10 ± 0.05
A1491	Ore-grade sphalerite	230,113		0.12 ± 0.01
A1975_465–468	Ore-grade sphalerite	333,067		0.10 ± 0.02
A1975_471–472	Ore-grade sphalerite	69,688		0.106 ± 0.001
A2191	Ore-grade sphalerite	401,653		0.10 ± 0.06
UBC-3-1A_WR	Exoskarn waste rock	6.34		0.15 ± 0.06

[a] δ^{66}Zn expressed relative to PCIGR-1 Zn.
[b] 2 SD for triplicate analysis on the MC-ICP-MS.

Wulfenite supersaturation was frequently observed in field barrels (Fig. 4), but its formation was usually limited by Pb availability: whenever Pb was measured above the detection limit of ICP-MS, wulfenite supersaturation typically ensued (Fig. 4). Pb solubility in aqueous solutions is exceedingly low due to its tendency to precipitate as sparingly soluble Pb-carbonate, Pb-sulfate, Pb-hydroxide or Pb-molybdate minerals (Conlan et al., 2012; Hem, 1976). The ample availability of dissolved anions such as HCO_3^-, SO_4^{2-} and OH^- in mine drainage therefore imparts competition for the association of MoO_4^{2-} anions and Pb^{2+} cations and limits wulfenite precipitation to Mo-rich fluids coming into contact with Pb-rich materials (Hirsche, 2012). Overall, powellite and wulfenite formation were unlikely to cause the observed Mo isotopic fractionation in mine drainage.

Ultimately, we propose that the shift towards heavier δ^{98}Mo in mine-drainage relative to the range found in solid-phase samples was most likely dominated by adsorption processes. The variations in δ^{98}Mo in molybdenites remain a source of uncertainty in interpreting mine drainage δ^{98}Mo values in small scale field weathering experiments. The role of secondary molybdate mineral precipitation in driving heavy Mo isotope compositions in mine drainage, if any, should be more easily assessed once fractionation factors for their formation are known. In addition, diverse microbiological communities are known to thrive in Antamina waste rock (Dockrey et al., 2014). The redox-active geochemistry of Mo and its activity in biological enzymes may result in biological fractionations (Wang, 2012) which are at present poorly understood. Finally, a better understanding of Mo isotopic fractionation during mineral dissolution would also be useful constrain to what

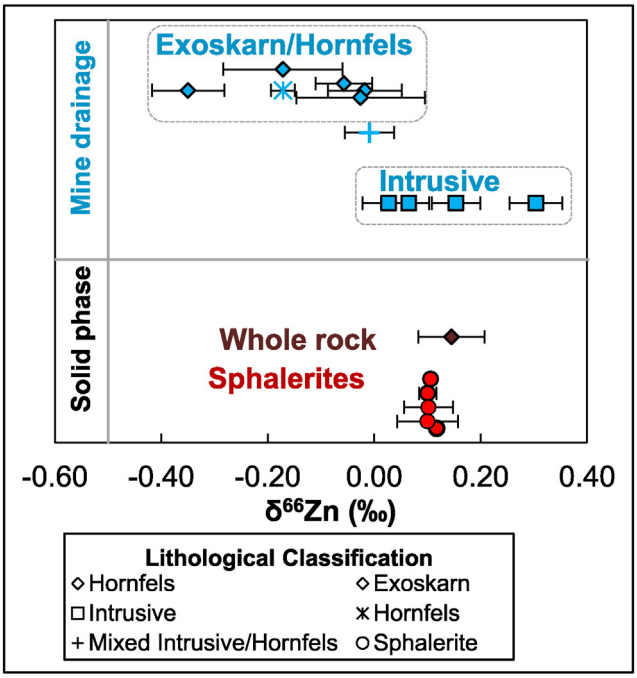

Fig. 5. Zinc isotopic compositions of mine drainage from experimental field barrels and waste rock piles, and of sphalerites and waste rock. Data are spread vertically for clarity. δ^{66}Zn is expressed relative to the PCIGR-1 Zn standard. Error bars are 2 SD for triplicate analysis on the MC-ICP-MS.

extent dissolution may have contributed to the heavier signatures observed in mine drainage.

4.2. Zinc stable isotope composition of waste rock, sphalerites and mine drainage

In contrast to the Mo isotopic heterogeneity among solid phase samples, remarkably little variations in Zn isotope ratios were observed among sphalerites with an average δ^{66}Zn of 0.11 ± 0.01‰ (2 SD, n = 5). In addition, the Zn isotopic composition of an exoskarn waste rock sample (UBC-3-1A) was indistinguishable from the value defined by Antamina sphalerites, lending further support for a source δ^{66}Zn value of 0.11‰. This provides a well-constrained isotopic signature for the source of Zn to Antamina mine drainage, which falls within the estimated global average Zn isotopic signature for sphalerites compiled by Sonke et al. (2008) of 0.05 ± 0.20‰ (expressed relative to our in-house PCIGR-1 Zn reference standard).

In mine drainage samples collected from field barrels and experimental waste rock piles, a span of 0.65‰ in δ^{66}Zn was observed (Table 2, Fig. 5). While this range in fractionation of 0.33‰ amu^{-1} was smaller than the range found for δ^{98}Mo in water samples (1.47‰ amu^{-1}), the extent of Zn isotope fractionation measured in solution was larger than results from previous studies of Zn isotopic compositions in mine drainage (Aranda et al., 2012; Borrok et al., 2009; Matthies et al., 2014a, 2014b). The homogeneous isotopic composition of Antamina sphalerites and the lack of substantial Zn isotopic fractionation during oxidative weathering of this mineral (Fernandez and Borrok, 2009) indicate that there are Zn attenuation processes in solution that induce Zn isotope fractionation in mine drainage.

δ^{66}Zn in mine drainage was associated with waste rock lithology and pH: drainage produced by weathering of carbonate-rich waste rock types (exoskarn, hornfels) was isotopically lighter with a range in δ^{66}Zn of −0.35 to −0.02‰, while carbonate-poor intrusive weathering produced mine drainage with a range of +0.03 to +0.30‰ (Fig. 5). When plotted against pH, lighter δ^{66}Zn values were found in neutral to alkaline waters (Fig. 6) that are associated with carbonate-rich waste rock weathering.

The shift towards lighter δ^{66}Zn in alkaline pH drainage coincides with conditions favorable to Zn attenuation processes, including adsorption onto Fe- and Mn-oxyhydroxide minerals (Balistrieri et al., 2008; Fuller and Bargar, 2014; Juillot et al., 2008) and calcite (Zachara et al., 1988), as well as formation of secondary Zn minerals such as $Zn(OH)_2$, Zn carbonates (e.g. smithsonite, hydrozincite) and amorphous Zn silicates (Wanty et al., 2013a). Mineral saturation indices computed for exoskarn and hornfels field barrels with light δ^{66}Zn compositions showed that the only secondary mineral that reached a state of supersaturation was hydrozincite (Fig. 7). Hydrozincite supersaturation occurred in hornfels and exoskarn-bearing waste rock drainage as a result of their greater carbonate and Zn content. Saturation indices of other Zn mineral groups including sulfates and hydroxysulfates were always significantly undersaturated. Because dissolved SiO_2 was not analyzed, it was impossible to calculate mineral SIs for Zn silicates.

Previous observations in the literature show that adsorption and hydrozincite formation are both plausible explanations for the shift to lighter δ^{66}Zn in alkaline-pH field barrel drainage. Experimental fractionation factors for Zn adsorption onto ferrihydrite, goethite, birnessite and carbonates are dominated by a preferential uptake of heavy Zn isotopes due to a change in coordination from octahedral aqueous Zn^{2+} ions to stiffer tetrahedral bonding in the sorbed phase, with fractionation factors ($\alpha_{solution\text{-}solid}$) ranging from 0.99984 to 0.99731 (Balistrieri

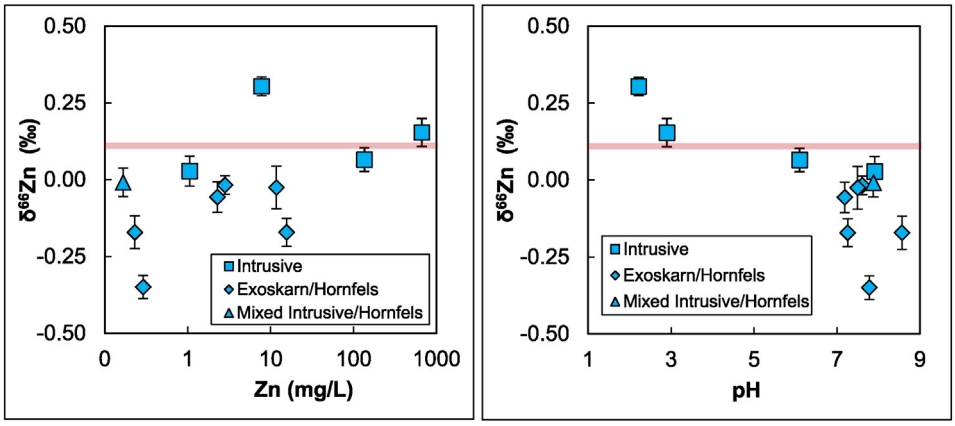

Fig. 6. Zinc isotope compositions in mine drainage collected from experimental field barrels and waste rock piles, expressed relative to zinc concentrations (left) and pH (right). Symbol shape indicates lithology in field barrel or pile, as in Fig. 4. Horizontal shadow shows the isotopic composition of Antamina sphalerites. δ^{66}Zn is expressed relative to the PCIGR-1 Zn standard. Error bars are 2 SD for triplicate analysis on the MC-ICP-MS.

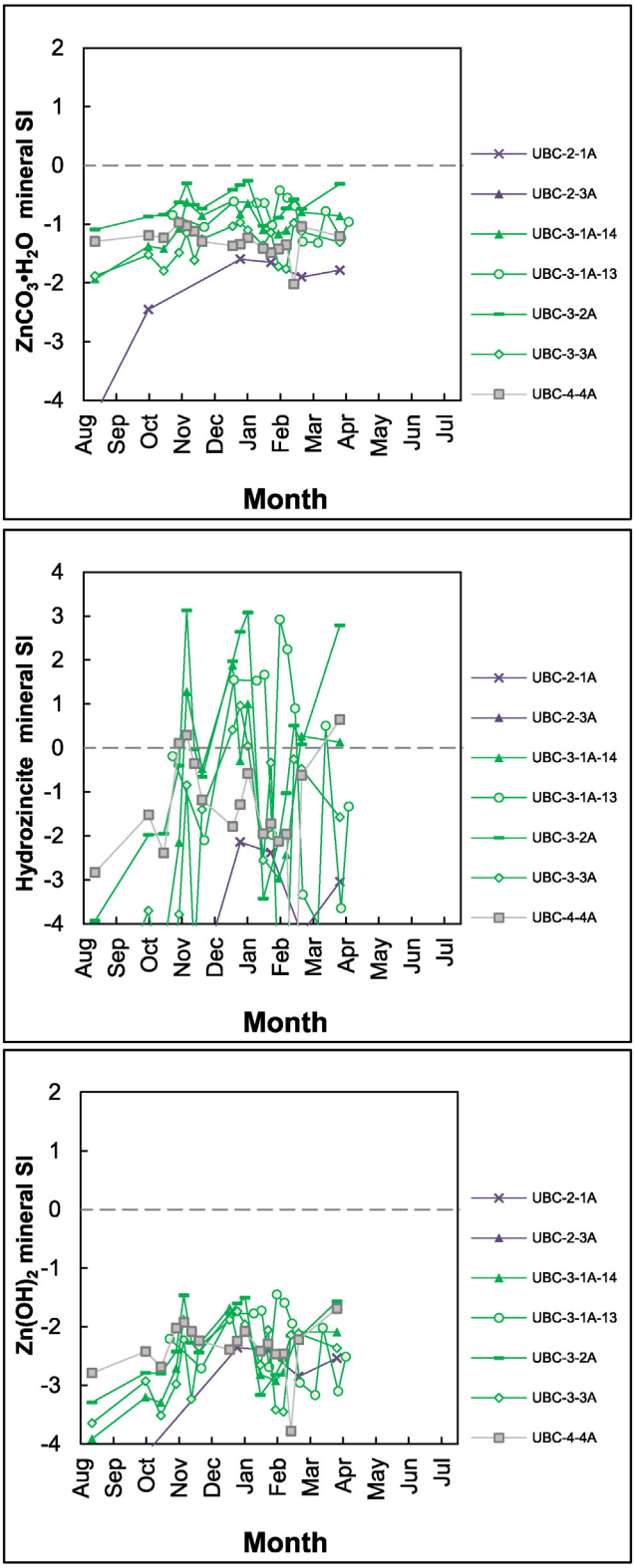

Fig. 7. Seasonal variation in $ZnCO_3 \cdot H_2O$ (top), hydrozincite (middle) and $Zn(OH)_2$ (bottom) mineral saturation indices (SI) in field barrel drainage calculated using PHREEQC. Data are shown for the entire rainy season during which a sample was drawn for Zn isotope analysis. Isotope sampling was conducted in April. All mineral SIs in field barrel UBC-2-3A fall below range shown on graph. Note difference in y-axis scales.

et al., 2008; Bryan et al., 2015; Dong and Wasylenki, 2014; Juillot et al., 2008). Abiotic and biologically-mediated hydrozincite precipitation also has similar fractionation factors to Zn adsorption, ranging from 0.99965 to 0.99982 (Veeramani et al., 2015; Wanty et al., 2013b). Oxyhydroxides and carbonates are ubiquitous during the weathering of sulfide and carbonate-rich waste mines (Al et al., 2000), and SEM imaging along with sequential chemical extractions of weathered waste rock collected in full-scale waste rock dumps at Antamina showed an association of Zn with carbonate and reducible (i.e. oxyhydroxide mineral) phases (Laurenzi et al., 2015) supporting the hypothesis that either or both of these processes can be responsible for Zn attenuation and associated isotopic fractionation.

In contrast, in acidic mine drainage conditions, δ^{66}Zn values exhibited variations of less than 0.2‰ relative to Antamina sphalerites (Fig. 6). Basal drainage from the intrusive waste rock pile contained the most elevated Zn concentrations (135–667 mg/L), and its isotopic composition was indistinguishable from the sphalerite values (Fig. 6). From these results, we infer that minimal Zn attenuation and isotopic fractionation is occurring under acidic pH conditions, and the mine drainage δ^{66}Zn value directly reflects the source, as has been reported in other studies of Zn isotopes in acid mine drainage (Matthies et al., 2014a, 2014b).

5. Implications for use of metal stable isotope ratios to monitor mine drainage geochemistry

Significant and resolvable fractionation of Mo and Zn isotope compositions was observed in waste rock drainage that was likely driven by attenuation processes. This makes these metal isotope ratios useful tools to monitor metal attenuation processes in mine waste dumps, in addition to conventional geochemical analyses. Future research should continue to provide more constraints on the processes that govern Mo and Zn isotope fractionation in environmentally-relevant reactions, including mineral dissolution, adsorption, secondary mineral formation and microbial processes.

Both of these elements show opposite isotopic fractionation responses during adsorption processes as a result of differences in coordination chemistry during complexation at the mineral-water interface (Wasylenki et al., 2011). Taken together, Mo and Zn isotope ratios may serve as informative precursors to evolving pH conditions within mine waste dumps, much in a way their concentration patterns provide information about pH (Dockrey and Stockwell, 2012). A localized drop in pH as a result of persistent sulfide oxidation and consumption of mineral buffering capacity would be reflected in enhanced Mo adsorption and a shift towards heavier δ^{98}Mo signatures in mine drainage. This pH drop would simultaneously result in dissolution of the isotopically heavy pool of accumulated secondary Zn in the form of adsorbed Zn and secondary Zn carbonate, hydroxide and/or silicate minerals (Matthies et al., 2014a; Veeramani et al., 2015; Wanty et al., 2013a, 2013b). δ^{66}Zn would therefore be predicted to shift towards a heavier δ^{66}Zn during the flushing of these secondary Zn phases before reaching a stable signature resembling the value of sphalerites once persistent ARD conditions have led to the exhaustion of secondary Zn minerals. Monitoring Mo and Zn isotope compositions in mine drainage could thereby provide useful information for transient changes in geochemical conditions within waste rock dumps that are otherwise difficult to assess from outflow concentration and pH measurements alone.

At this point, the application of Zn isotope ratios as a tracer for attenuation processes is simplified in contrast to Mo isotopes due to the lack of Zn isotopic heterogeneity in the primary solid phase. In acidic conditions, Zn isotope ratios are representative of source (sphalerite) isotopic composition with little effect of secondary processes. However, in neutral to alkaline mine drainage, heavy Zn isotopes are preferentially removed, likely by adsorption and/or precipitation of secondary zinc carbonates, making Zn isotope ratios indicators of Zn attenuation.

Isotope fractionations in mine drainage for Mo are larger than Zn. The application of Mo isotope compositions as a tracer of attenuation processes is complicated by the isotopic heterogeneity of molybdenites in waste rock. Despite this heterogeneity, δ^{98}Mo measurements in mine drainage provide evidence for Mo attenuation, as demonstrated by the

accumulation of heavy Mo isotopes in solution. The dominant Mo attenuation process that can be resolved at present in mine drainage using Mo isotopes is adsorption, although future studies of Mo isotopes should improve our ability to consider the role of other relevant Mo attenuation processes (e.g. metal molybdate precipitation), and constrain uncertainties associated with the mechanisms and magnitude of isotopic fractionation during molybdenite weathering.

The application of metal isotope ratios to track metal attenuation in mine drainage is still in its infancy, but the observations in this study and in previous studies (Aranda et al., 2012; Borrok et al., 2009, 2008; Matthies, 2015; Matthies et al., 2014a, 2014b) indicate their potential as powerful geochemical tracers in contaminated environments. Further constraints on the mechanisms of Mo and Zn isotopic fractionation in laboratory experiments and under field conditions should make Mo and Zn isotope ratios insightful tracers of geochemical processes occurring in a variety of subsurface environments including – but not limited to – mine waste dumps that are typically inaccessible for discrete sampling.

Acknowledgments

K. Gordon, V. Lai and Dr. M. Amini are thanked for their assistance in operating the MC-ICP-MS and ICP-MS at PCIGR. K. Gordon and A. Shiel are thanked for the intercalibration of Zn isotope standards. B. Harrison, M. Lorca-Ugalde, M. St-Arnault and L. Laurenzi assisted with sample collection along with Antamina field staff. The authors also wish to thank the Editor, and R.M. Mathur and two anonymous reviewers for comments which improved this manuscript. Funding was provided by an NSERC Canada Graduate Scholarship to E.K.S and by an NSERC Collaborative Research and Training Experience grant (CREATE-MAGNET) (413976-2012) to D.W. and K.U.M., and by the Compañía Minera Antamina. Solid-phase mineralogy by XRD was compiled from the theses of J. Dockrey (MSc) and Dr. H. Peterson (PhD) with analytical support from Dr. E. Pani and Jenny Lai.

Appendix A. Supplementary data

Supplementary data to this article can be found online at http://dx.doi.org/10.1016/j.scitotenv.2016.01.053.

References

Achary, S.N., Patwe, S.J., Mathews, M.D., Tyagi, A.K., 2006. High temperature crystal chemistry and thermal expansion of synthetic powellite (CaMoO4): a high temperature X-ray diffraction (HT-XRD) study. J. Phys. Chem. Solids 67, 774–781.
Al, T.A., Martin, C.J., Blowes, D.W., 2000. Carbonate-mineral/water interactions in sulfide-rich mine tailings. Geochim. Cosmochim. Acta 64, 3933–3948.
Amos, R.T., Blowes, D.W., Bailey, B.L., Sego, D.C., Smith, L., Ritchie, A.I.M., 2015. Waste-rock hydrogeology and geochemistry. Appl. Geochem. 57, 140–156.
Aranda, C., 2010. Assessment of Waste Rock Weathering Characteristics at the Antamina Mine Based on Field Cell Experiments. University of British Columbia (MASc thesis, 260 pp.).
Aranda, S., Borrok, D.M., Wanty, R.B., Balistrieri, L.S., 2012. Zinc isotope investigation of surface and pore waters in a mountain watershed impacted by acid rock drainage. Sci. Total Environ. 420, 202–213.
Archer, C., Vance, D., 2008. The isotopic signature of the global riverine molybdenum flux and anoxia in the ancient oceans. Nat. Geosci. 1, 597–600.
Balistrieri, L.S., Borrok, D.M., Wanty, R.B., Ridley, W.I., 2008. Fractionation of Cu and Zn isotopes during adsorption onto amorphous Fe(III) oxyhydroxide: experimental mixing of acid rock drainage and ambient river water. Geochim. Cosmochim. Acta 72, 311–328.
Barceloux, D.G., 1999. Molybdenum. Clin. Toxicol. 37, 231–237.
Barling, J., Anbar, A.D., 2004. Molybdenum isotope fractionation during adsorption by manganese oxides. Earth Planet. Sci. Lett. 217, 315–329.
Bay, D.S., 2009. Hydrological and Hydrogeochemical Characteristics of Neutral Drainage From a Waste Rock Test Pile. University of British Columbia (MSc Thesis, 331 pp.).
Ramana, C.V., Becker, U., Shutthanandan, V., Julien, C.M., 2008. Oxidation and metal-insertion in molybdenite surfaces: evaluation of charge-transfer mechanisms and dynamics. Geochem. Trans. 9, 8.
Beckie, R.D., Aranda, C., Blackmore, S.R., Peterson, H.E., Hirsche, T., Javadi, M., Blaskovich, R., Haupt, C., Conlan, M., Bay, D., Harrison, B., Brienne, S., Klein, B., Mayer, K.U., 2011. A study of the mineralogical, hydrological and biogeochemical controls on drainage from waste rock at the Antamina Mine, Peru: an overview. Proceedings of the Tailings and Mine Waste Conference, Vancouver, Canada, November 6–9, 2011.
Blackmore, S., Smith, L., Ulrich Mayer, K., Beckie, R.D., 2014. Comparison of unsaturated flow and solute transport through waste rock at two experimental scales using temporal moments and numerical modeling. J. Contam. Hydrol. 171, 49–65.
Borrok, D.M., Nimick, D.A., Wanty, R.B., Ridley, W.I., 2008. Isotopic variations of dissolved copper and zinc in stream waters affected by historical mining. Geochim. Cosmochim. Acta 72, 329–344.
Borrok, D.M., Wanty, R.B., Ian Ridley, W., Lamothe, P.J., Kimball, B.A., Verplanck, P.L., Runkel, R.L., 2009. Application of iron and zinc isotopes to track the sources and mechanisms of metal loading in a mountain watershed. Appl. Geochem. 24, 1270–1277. http://dx.doi.org/10.1016/j.apgeochem.2009.03.010.
Bryan, A.L., Dong, S., Wilkes, E.B., Wasylenki, L.E., 2015. Zinc isotope fractionation during adsorption onto Mn oxyhydroxide at low and high ionic strength. Geochim. Cosmochim. Acta 157, 182–197.
Canadian Council of Ministers of the Environment, 1999. Canadian Soil Quality Guidelines for the Protection of Environmental and Human Health — Zinc.
Conlan, M.J.W., Mayer, K.U., Blaskovich, R., Beckie, R.D., 2012. Solubility controls for molybdenum in neutral rock drainage. Geochem. Explor. Environ. Anal. 12, 21–32.
Connelly, J.N., Ulfbeck, D.G., Thrane, K., Bizzarro, M., Housh, T., 2006. A method for purifying Lu and Hf for analyses by MC-ICP-MS using TODGA resin. Chem. Geol. 233, 126–136.
Cora, I., Czugler, M., Dódony, I., Rečnik, A., 2011. On the symmetry of wulfenite (Pb[MoO4]) from Mežica (Slovenia). Acta Crystallogr. Sect. C: Cryst. Struct. Commun. 67, 33–35.
Corazao Gallegos, J.C., 2007. The Design, Construction, Instrumentation and Initial Response of a Field-scale Waste Rock Pile Experiment. University of British Columbia (MASc Thesis, 247 pp).
Dockrey, J.W., 2010. Microbiology and Geochemistry of Neutral pH Waste Rock From the Antamina Mine, Peru. University of British Columbia (MSc Thesis, 225 pp.).
Dockrey, J.W., Stockwell, J.S., 2012. Early indicators of acid seepage generation — a comparative study of long-term seepage quality from two waste rock dumps in the Central Rocky Mountains. Proceedings of the 9th International Conference on Acid Rock Drainage, May, pp. 20–25 (Ottawa, Canada).
Dockrey, J., Lindsay, M., Mayer, K., Beckie, R., Norlund, K., Warren, L., Southam, G., 2014. Acidic microenvironments in waste rock characterized by neutral drainage: bacteria–mineral interactions at sulfide surfaces. Minerals 4, 170–190.
Dong, S., Wasylenki, L.E., 2014. Zinc isotope fractionation during adsorption and incorporation with calcite, Goldschmidt. Geochim. Cosmochim. Acta 84, 3943.
Fernandez, A., Borrok, D.M., 2009. Fractionation of Cu, Fe, and Zn isotopes during the oxidative weathering of sulfide-rich rocks. Chem. Geol. 264, 1–12.
Fuller, C.C., Bargar, J.R., 2014. Processes of zinc attenuation by biogenic manganese oxides forming in the hyporheic zone of Pinal Creek, Arizona. Environ. Sci. Technol. 48, 2165–2172.
Goldberg, S., Forster, H.S., Godfrey, C.L., 1996. Molybdenum adsorption on oxides, clay minerals, and soils. Soil Sci. Soc. Am. J. 60, 425.
Goldberg, T., Archer, C., Vance, D., Poulton, S.W., 2009. Mo isotope fractionation during adsorption to Fe (oxyhydr)oxides. Geochim. Cosmochim. Acta 73, 6502–6516.
Goldberg, T., Gordon, G., Izon, G., Archer, C., Pearce, C.R., McManus, J., Anbar, A.D., Rehkämper, M., 2013. Resolution of inter-laboratory discrepancies in Mo isotope data: an intercalibration. J. Anal. At. Spectrom. 28, 724–735.
Greber, N.D., Hofmann, B.A., Voegelin, A.R., Villa, I.M., Nägler, T.F., 2011. Mo isotope composition in Mo-rich high- and low-T hydrothermal systems from the Swiss Alps. Geochim. Cosmochim. Acta 75, 6600–6609.
Greber, N.D., Pettke, T., Nägler, T.F., 2014. Magmatic–hydrothermal molybdenum isotope fractionation and its relevance to the igneous crustal signature. Lithos 190-191, 104–110.
Greber, N.D., Puchtel, I.S., Nägler, T.F., Mezger, K., 2015. Komatiites constrain molybdenum isotope composition of the Earth's mantle. Earth Planet. Sci. Lett. 421, 129–138.
Gupta, R.K., Van Den Elshout, S., Abrol, I.P., 1987. Effect of pH on zinc adsorption–precipitation reactions in an alkali soil. Soil Sci. 143, 198–204.
Gustafsson, J.P., 2003. Modelling molybdate and tungstate adsorption to ferrihydrite. Chem. Geol. 200, 105–115.
Hall, G.E.M., Vaive, J.E., Beer, R., Hoashi, M., 1996. Selective leaches revisited, with emphasis on the amorphous Fe oxyhydroxide phase extraction. J. Geochem. Explor. 56, 59–78.
Hannah, J.L., Stein, H.J., Wieser, M.E., de Laeter, J.R., Varner, M.D., 2007. Molybdenum isotope variations in molybdenite: vapor transport and Rayleigh fractionation of Mo. Geology 35, 703–706.
Hem, J.D., 1976. Inorganic chemistry of lead in water, in: lead in the environment. In: Lovering, T.G. (Ed.), U.S. Geological Survey Professional Paper 957, pp. 5–11.
Hirsche, D.T., 2012. A Field and Humidity Cell Study of Metal Attenuation in Neutral Rock Drainage From the Antamina Mine, Peru. University of British Columbia (MSc Thesis, 152 pp.).
Iavazzo, P., Adamo, P., Boni, M., Hillier, S., Zampella, M., 2012. Mineralogy and chemical forms of lead and zinc in abandoned mine wastes and soils: an example from Morocco. J. Geochem. Explor.
Jacquat, O., Voegelin, A., Villard, A., Marcus, M.A., Kretzschmar, R., 2008. Formation of Zn-rich phyllosilicate, Zn-layered double hydroxide and hydrozincite in contaminated calcareous soils. Geochim. Cosmochim. Acta 72, 5037–5054.
Johansson, G., Caminiti, R., 1986. The hydration of tungstate and molybdate ions in aqueous solution. Z. Naturforsch. 41a, 1325–1329.
Juillot, F., Maréchal, C., Ponthieu, M., Cacaly, S., Morin, G., Benedetti, M., Hazemann, J.L., Proux, O., Guyot, F., 2008. Zn isotopic fractionation caused by sorption on goethite and 2-lines ferrihydrite. Geochim. Cosmochim. Acta 72, 4886–4900.
Kaback, D.S., 1976. Transport of molybdenum in mountainous streams, Colorado. Geochim. Cosmochim. Acta 40, 581–582.

Laurenzi, L., Mayer, K.U., Beckie, R., 2015. A metal attenuation study on waste rock collected from the East Dump, Antamina Mine, Peru: a combined mineralogical and geochemical approach. Int. Conf. Acid Rock Drainage, April 2015, Santiago Chile.
Liermann, L.J., Mathur, R., Wasylenki, L.E., Nuester, J., Anbar, A.D., Brantley, S.L., 2011. Extent and isotopic composition of Fe and Mo release from two Pennsylvania shales in the presence of organic ligands and bacteria. Chem. Geol. 281, 167–180.
Lipten, E.J., Smith, S.W., 2004. The geology of the antamina copper–zinc deposit, Peru, South America. In: Porter, T.M. (Ed.), Super Porphyry Copper & Gold Deposits: A Global Perspective. PGC Publishing, Adelaide, Australia.
Lugli, C., Medici, L., Saccardo, D., 1999. Natural wulfenite: structural refinement by single-crystal X- ray diffraction. N. Jb. Mineral. 281–288.
Maréchal, N., Télouk, P., Albarède, F., 1999. Precise analysis of copper and zinc isotopic compositions by plasma-source mass spectrometry. Chem. Geol. 156, 251–273.
Mathur, R., Brantley, S., Anbar, A.D., Munizaga, F., Maksaev, V., Newberry, R., Vervoort, J., Hart, G., 2010. Variation of Mo isotopes from molybdenite in high-temperature hydrothermal ore deposits. Mineral. Deposita 45, 43–50.
Matthies, R., 2015. Application of heavy stable isotopes in mine water research. Rev. Environ. Sci. Biotechnol. 14, 5–8.
Matthies, R., Krahé, L., Blowes, D.W., 2014a. Zinc stable isotope fractionation upon accelerated oxidative weathering of sulfidic mine waste. Sci. Total Environ. 487, 97–101.
Matthies, R., Sinclair, S.A., Blowes, D.W., 2014b. The zinc stable isotope signature of waste rock drainage in the Canadian permafrost region. Appl. Geochem. 48, 53–57.
Nägler, T.F., Neubert, N., Böttcher, M.E., Dellwig, O., Schnetger, B., 2011. Molybdenum isotope fractionation in pelagic euxinia: evidence from the modern Black and Baltic Seas. Chem. Geol. 289, 1–11.
Nägler, T.F., Anbar, A.D., Archer, C., Goldberg, T., Gordon, G.W., Greber, N.D., Siebert, C., Sohrin, Y., Vance, D., 2014. Proposal for an international molybdenum isotope measurement standard and data representation. Geostand. Geoanal. Res. 38, 149–151.
Nakagawa, Y., Takano, S., Firdaus, M., 2012. The molybdenum isotopic composition of the modern ocean. Geochem. J. 46, 131–141.
Neubert, N., Heri, A.R., Voegelin, A.R., Nägler, T.F., Schlunegger, F., Villa, I.M., 2011. The molybdenum isotopic composition in river water: constraints from small catchments. Earth Planet. Sci. Lett. 304, 180–190.
Parkhurst, D.L., Appelo, C.A.J., 2013. Description of input and examples for PHREEQC version 3 — a computer program for speciation, batch-reaction, one-dimensional transport, and inverse geochemical calculations. U.S. Geological Survey Techniques and Methods, Book 6, Chapter A43 497 pp.
Peterson, H.E., 2014. Unsaturated Hydrology, Evaporation and Geochemistry of Neutral and Acid Rock Drainage in the Highly Heterogeneous Mine Waste Rock at the Antamina Mine, Peru. University of British Columbia (PhD Thesis, 345 pp.).
Preis, W., Gamsjäger, H., 2001. (Solid + solute) phase equilibria in aqueous solution. XIII. Thermodynamic properties of hydrozincite and predominance diagrams for (Zn^{2+} + H_2O + CO_2). J. Chem. Thermodyn. 33, 803–819.
Sahu, K.C., Prusty, B.G., Godgul, G., 1994. Metal contamination due to mining and milling activities at the Zawar zinc mine, Rajasthan, India. Chem. Geol. 112, 293–307.
Schauble, E.A., 2004. Applying stable isotope fractionation theory to new systems. Rev. Mineral. Geochem. 55, 65–111.
Shiel, A.E., Barling, J., Orians, K.J., Weis, D., 2009. Matrix effects on the multi-collector inductively coupled plasma mass spectrometric analysis of high-precision cadmium and zinc isotope ratios. Anal. Chim. Acta 633, 29–37.
Shiel, A.E., Weis, D., Cossa, D., Orians, K.J., 2013. Determining provenance of marine metal pollution in French bivalves using Cd, Zn and Pb isotopes. Geochim. Cosmochim. Acta 121, 155–167.
Siebert, C., Nägler, T.F., von Blanckenburg, F., Kramers, J.D., 2003. Molybdenum isotope records as a potential new proxy for paleoceanography. Earth Planet. Sci. Lett. 211, 159–171.
Skierszkan, E.K., Amini, M., Weis, D., 2015. A practical guide for the design and implementation of the double-spike technique for precise determination of molybdenum isotope compositions of environmental samples. Anal. Bioanal. Chem. 407, 1925–1935.
Sonke, J., Sivry, Y., Viers, J., Freydier, R., Dejonghe, L., Andre, L., Aggarwal, J., Fontan, F., Dupre, B., 2008. Historical variations in the isotopic composition of atmospheric zinc deposition from a zinc smelter. Chem. Geol. 252, 145–157.
Valko, M., Morris, H., Cronin, M.T.D., 2005. Metals, toxicity and oxidative stress. Curr. Med. Chem. 12, 1161–1208.
Veeramani, H., Eagling, J., Jamieson-Hanes, J.H., Kong, L., Ptacek, C.J., Blowes, D.W., 2015. Zinc isotope fractionation as an indicator of geochemical attenuation processes. Environ. Sci. Technol. Lett. 314–319.
Voegelin, A.R., Nägler, T.F., Pettke, T., Neubert, N., Steinmann, M., Pourret, O., Villa, I.M., 2012. The impact of igneous bedrock weathering on the Mo isotopic composition of stream waters: natural samples and laboratory experiments. Geochim. Cosmochim. Acta 86, 150–165.
Wang, D., 2012. Redox chemistry of molybdenum in natural waters and its involvement in biological evolution. Front. Microbiol. 3, 1–7.
Wanty, R.B., De Giudici, G., Onnis, P., Rutherford, D., Kimball, B.A., Podda, F., Cidu, R., Lattanzi, P., Medas, D., 2013a. Formation of a low-crystalline Zn-silicate in a stream in SW Sardinia, Italy. Procedia Earth and Planetary Science. Elsevier B.V., pp. 888–891.
Wanty, R.B., Podda, F., De Giudici, G., Cidu, R., Lattanzi, P., 2013b. Zinc isotope and transition-element dynamics accompanying hydrozincite biomineralization in the Rio Naracauli, Sardinia, Italy. Chem. Geol. 337-338, 1–10.
Wasylenki, L.E., Rolfe, B.A., Weeks, C.L., Spiro, T.G., Anbar, A.D., 2008. Experimental investigation of the effects of temperature and ionic strength on Mo isotope fractionation during adsorption to manganese oxides. Geochim. Cosmochim. Acta 72, 5997–6005.
Wasylenki, L.E., Weeks, C.L., Bargar, J.R., Spiro, T.G., Hein, J.R., Anbar, A.D., 2011. The molecular mechanism of Mo isotope fractionation during adsorption to birnessite. Geochim. Cosmochim. Acta 75, 5019–5031.
Wiederhold, J.G., 2015. Metal stable isotope signatures as tracers in environmental geochemistry. Environ. Sci. Technol. (150217161826001).
Wieser, M.E., de Laeter, J.R., 2003. A preliminary study of isotope fractionation in molybdenites. Int. J. Mass Spectrom. 225, 177–183.
Xu, N., Christodoulatos, C., Braida, W., 2006. Adsorption of molybdate and tetrathiomolybdate onto pyrite and goethite: effect of pH and competitive anions. Chemosphere 62, 1726–1735.
Yang, J., Siebert, C., Barling, J., Savage, P., Liang, Y.-H., Halliday, A.N., 2015. Absence of molybdenum isotope fractionation during magmatic differentiation at Hekla volcano, Iceland. Geochim. Cosmochim. Acta 162, 126–136.
Zachara, J., Kittrick, J., Harsh, J., 1988. The mechanism of Zn^{2+} adsorption on calcite. Geochim. Cosmochim. Acta 52, 2281–2291.